International Journal of Biological Macromolecules 154 (2020) 1324–1331

Contents lists available at ScienceDirect

International Journal of Biological Macromolecules

journal homepage: www.elsevier.com/locate/ijbiomac

Preparation and characterization of bioactive silk fibroin/paramylon blend films for chronic wound healing

R. Arthe [a], D. Arivuoli [a,*], Venkatraman Ravi [b]

[a] Crystal Growth Centre, Anna University, Chennai, India
[b] Department of Microbiology and Cell Biology, Indian Institute of Science, Bengaluru, India

ARTICLE INFO

Article history:
Received 20 June 2019
Received in revised form 3 November 2019
Accepted 3 November 2019
Available online 13 November 2019

Keywords:
Silk fibroin
Paramylon
Extra cellular matrix
Thermal properties
Mechanical properties

ABSTRACT

A major challenge in the chronic wound healing is a self-care wound dressing. The problem in chronic wounds is the lack of functional extracellular matrix to stimulate healing. The extracellular matrix is a network of proteins and polysaccharides that serves as physical framework and provides regulatory signals. The primary goal is to mimic the property of the extracellular matrix with Silk Fibroin and Paramylon to produce a novel bioactive film. Silk fibroin is a fibrous protein having unique mechanical properties and tunable biodegradability that makes it favourable for tailoring to specific applications. Paramylon is a β-glucan that possess a broad spectrum of biological activity that enhances the immune response. Silk fibroin/paramylon blend films have been prepared by solution casting and were examined for structural, thermal, mechanical and other physical properties for knowing its transformation for chronic wound healing. It was observed that the fibroin films shows high thermal stability, high hydrophobicity, high stiffness value whereas the paramylon film show good water absorption property and both fibroin and paramylon shows good blood compatibility and was non-toxic as well. It also confirms that the blended films showed a combination of fibroin and paramylon property at different concentrations without any chemical interaction.

1. Introduction

Chronic wounds are increasing problem all over the world as the population grows older and the incidence of liable chronic states, such as diabetes, becomes epidemic [1]. The Life of patients with chronic wounds is greatly compromised, as the life expectancy in major cases is reportedly reduced to as little as 5 years, the mortality can be worse than many common cancers [2]. This failure results in chronic wounds have directed the focus to the extracellular matrix (ECM) whose defectiveness contributed to the delay in chronic wounds [3]. Extracellular matrix based biomaterials have an established place for wound healing and tissue regeneration. Biomaterials play a major role in providing three-dimensional scaffold and artificial extracellular-matrix environments for tissue regeneration [4].

The extracellular matrix is the bulkiest component of the dermal layer and the synthesis of extracellular matrix plays a key role in the process of wound healing especially in chronic wounds. Extracellular matrix is made up of collagen and an elastic fibers dispersed in glycosaminoglycans, proteoglycans and connective tissue glycoprotein [5]. Proteins and Polysaccharides were the most important components of extracellular matrix in dermal tissue [6]. Hence in the present study we tend to mimic the extracellular-matrix for the improvement of chronic wound heal with Silk fibroin (SF) and Paramylon (BG) blends.

Silk fibroin is a natural fibrous polymer that is derived from silkworms, spiders and other insects. Each silk fibre is composed of two sub-fibers, where fibroin is the core and two cores are coated and wrapped together with the glue-like protein called sericin [7]. Silk sericinisantigenic and elicits a strong allergic reactions. Hence the sericin protein may be removed from the fibroin by degumming process. Prasong et al. [8] proved that the silk without sericin has higher thermal stability than the silk with sericin and the process of sericin removing may enhances the crystalline formation by changing the structure from random coil to β-sheet conformation.

Silk Fibroin is one of the major protein of silk fibre which is reported to be a good substrate for cell adhesion and proliferation. It plays a major role in biomaterials due to its well known properties such as high tensile strength, controlled biodegradability, non-inflammatory characteristics and so on [9]. Regenerated silk films

* Corresponding author.
E-mail address: arivuoli@annauniv.edu (D. Arivuoli).

https://doi.org/10.1016/j.ijbiomac.2019.11.010
0141-8130/

are already used effectively to promote angiogenesis thereby helping in wound healing process [10,11]. The fibroin protein is known for wound dressing by regulating exudates of wound providing moist environment facilitating re-epithelialization and collagenisation [12]. Silk fibroin with various natural and synthetic polymers can be processed into biomaterials for a number of tissue engineering applications and also such blending can improve the property of silk fibroin by modulating the biodegradation rates and mechanical property [13]. Silk Fibroin can be prepared in various forms like gel, powder, film, matrix or fiber depending on the various applications from cosmetics till medical application.

Beta glucan is a fiber-type complex sugar derived from the cell wall of plants fungi, algae and few bacteria. Natural (1,3)-β-D-glucans are structurally complex homopolymer of glucose from yeast, grain and mushrooms which are well-known biological response modifiers [14]. BG have been extensively used in immunological and pharmacological studies and also in the field of nutritional supplements. Earlier invitro studies have proved that the macrophages have a specific binding receptor for β-glucans and upon activation by β-glucans this receptor stimulates a cascade of events leading the production of cytokines and other soluble factors secreted by the cells of the lymphoid system [15].

Studies conducted over the past decade have shown that BG inhibit tumor development [16], enhance defense against bacterial infection [17], activate macrophages [14], induce production of cytokines [18], are effective against burns, improve wound healing process by inducing the macrophage to release wound growth factors and lower serum lipids [19].

β-glucan currently used in nutritional supplements are from *Saccharomyces cerevisae*, but it is wide spread in nature ie., being found higher in plants, bacteria, fungi and algae. (1,3)-β-Glucan and its related glucans are important both as storage and structural polysaccharide in protozoans and chromistans [20]. Over the past few years, efforts have been directed towards the characterization of the properties and the functions of BG synthases from these organisms. But most of the BG synthases are membrane associated complexes and are difficult to purify and characterize due to their inherent instability after solubilization from their native membrane environment [21].

All the enzyme complexes producing BG in plants, bacteria and yeast are known to be present in the plasma membrane and secrete the BG either into the cell wall or outside the cell. Therefore utilization by the biotechnology industry is difficult as such proteins are only often active when present within the membrane rather than in soluble fraction. The protist*Euglenagracilis*, however manufactures an intracellular granular reserve BG in high amounts [22]. Because this reserve carbohydrate is granular and the enzymes synthesizing would be soluble rather than present in the membrane and thus these glucan synthases would be easier to use from a biotechnological point of view. They could be expressed in microorganisms and the carbohydrate isolated after growth in bioreactors. According to the yield and extraction procedures, BG from *Euglena gracilis* is economical for the wound dressing application.

Paramylon is β-(1,3)-D-glucan extracted from *Euglena gracilis* which yields paramylon of about 60–70% of the total dried cell [23]. Paramylon shows cytokine-related immunopotentiatingactivity [24]. Sulfated derivatives of paramylon and N,N-dimethylami noethylparamylon exhibit anti-human immunodeficiency virus (HIV) and antimicrobial effects [25]. In addition to the immune cell interaction, BG also interacts with the fibroblasts. Wei et al. [26] proved that BG directly helps in collagen biosynthesis by activation of transcription factors in normal human dermal fibroblasts. It is also reported to enhance the wound healing in animals subjected to skin incision, colon anastomosis and burns. Depending on the route of administration, β-glucan enhances wound healing by increasing macrophage infiltration and collagen deposition, by inducing tissue granulation and by enhancing reepithelialization [27].

In the present study, two natural polymers are blended to form a cost effective and a single interactive and bioactive wound dressing for the chronic wound healing.

2. Experimental

2.1. Materials

Bombyxmori silk cocoons were kindly supplied by the Department of studies in Sericulture sciences, University of Mysore. β (1-3)-D-glucan used were derived from *Euglena gracilis* and was purchased from Sigma-Aldrich chemical Co.(St. Louis, MO.) and used without further treatment. All the other chemicals used were analytical grade obtained commercially.

2.2. Extraction of silk fibroin from Bombyxmori Cocoon (bivoltine, white shell)

Regenerated aqueous silk fibroin solution was prepared by the Rockwood et al. 2011 [28]. Firstly, the *Bombyxmori* cocoons were cut into small pieces and treated with the boiling solution of 0.02 M Sodium Carbonate for 30 min under constant stirring for removing the core protein sericin from fibroin. During the process, small amount of cocoons were taken after 5, 10, 15 and 20 min to check the removal of sericin protein at regular intervals which were observed by SEM. Then the degummed fibres were washed 2 to 3 times with ultrapure water to remove the glue like sericin protein completely and dried overnight in a sterile condition. The degummed fibres were dissolved in 9.3 M Lithium Bromide (LiBr) for 4 h at 60 °C, yielding 20% (w/v) solution which is then dialysed against sterilized water for three days, changing water every 6 h in order to remove LiBr. After dialysis, the regenerated silk fibroin solution was kept under −20 °C followed by lyophilization at −110° for 36 h.

2.3. Preparation of FG blend films

The blends were formed by making 1% solution by weight with formic acid. The solutions were taken in five different ratios as 1/0, 0.75/0.25, 0.5/0.5, and 0.25/0.75, 0/1 of Silk Fibroin to Beta-glucan powder to form five groups which are coded as SF , FG 75:25, FG 50:50, FG 25:75 and BG respectively. All the solutions were stirred for 4 h using magnetic stirrer to form a clear solution before casting in polystyrene plates. The plates were then left in oven at 40 °C for 48 h to obtain SF, BG and SF/BG blend films.

2.4. Scanning electron microscopy (SEM)

Surface morphology of the films was observed using Carl Zeiss MA15/EVO 18 SEM. For SEM, The films were first cut into small pieces and then mounted on the stub with double side carbon tapes. The samples were then sputter coated with gold to enhance surface conductivity.

2.5. Contact angle measurement

The static contact angles of the films were measured at room temperature by the drop method using an optical contact angle meter to examine the film surface wettability. The substrates used for the experiments were glass microscope slide. Each slide is cleaned before use by soaking in ethanol overnight. 7 μL of distilled water was carefully injected on the film surface before measuring

and the measurement time was 24 s. The contact angles were measured on both sides of the drop and averaged.

2.6. Fourier transform infrared spectroscopy analysis (FTIR)

Secondary structure and conformational changes of the blend films were confirmed by FTIR spectroscopy with air as the reference in the spectral range of 4000–400 cm^{-1} at 4 cm^{-1} spectral resolution and 32 scans using JASCO International Co./Japan Fourier transform infrared Spectrometer Model FTIR-6300 instrument.

2.7. X-ray diffraction studies

Change in the crystalline nature upon blending SF and BG were studied by XRD. The films were cut to 1 cm by 1 cm in size and were placed in the sample holder. A scanning rate of 0.2 min and diffraction angle from 5° to 70° were taken.

2.8. Nanoindendation studies for stiffness

Measurements of stiffness on the fibroin blend samples were conducted using SPM coupled nanoindenter operated in force mode. Force-distance curves for each sample were measured at least 5 times in each different region, and the calculated stiffness was averaged and standard deviation determined. It is used to measure the hardness/modulus or elasticity of materials with resolution of nanometers, similar to conventional compression tests using Hysitron TI950 Triboindenter.

2.9. Degradation studies

2.9.1. Thermogravimetric analysis (TGA)

The thermal degradation of the SF/BG films was determined by thermogravimetric instrument at a heating rate of 10 °C/min and nitrogen gas flow rate at 50 ml/min.

2.9.2. Water absorption capacity

Water absorption capacity of the SF, BG & FG films was determined by immersion of films of known weight in Phosphate buffer saline (PBS) of pH 7.4 at room temperature for 24 h. The swollen weight (W_s) and dry weight (W_d, after drying) were measured. Then, the swelling index (SI) was calculated with the below formula

$$SI = \{(W_s - W_d)/W_s\} \times 100$$

2.9.3. In vitro enzyme degradation

Degradation of SF, BG & FG films were determined as percentage of weight remained after incubation in lysozyme enzyme solution for about 4 weeks. The films with known dry weight before degradation (W_0) were immersed in PBS (pH 7.4) containing 10 μg/mL lysozyme at room temperature for four weeks which was refreshed weekly. At various time intervals (1, 2, 3 & 4 weeks, the films were removed and dried overnight. The weight of the dried films is the weight after degradation (W_t). The percentage of the weight remained after degradation was analyzed using the formula below [29].

$$\%\,\text{Weight remained} = (W_t/W_0) \times 100$$

2.10. Blood compatibility testing – in vitro hemolytic activity of the films

Hemolysis activity assay was conducted to evaluate the blood compatibility of the blended films. In this experiment, a dry film was equilibrated in saline water (0.9% NaCl solution) for 24 h at 37 °C. Healthy Human ACD blood (0.25 ml) was added onto the wet films. After 20 min, 2.0 ml of saline was added onto the films to stop hemolysis and the test samples were incubated for 60 min at room temperature. Positive and negative controls were obtained by adding 0.25 ml Human ACD into distilled water and saline solution respectively. Incubated films were centrifuged at 4 °C (1500 rpm, 5 min), the supernatant was taken and its absorbance at 545 nm was recorded. The % hemolysis was calculated using the following equation [30,31]

$$\text{Hemolysis}\ (\%) = \left[\left(A_{\text{test sample}} - A_{(-)\ \text{control}}\right)/\left(A_{(+)\ \text{control}} - A_{(-)\ \text{control}}\right)\right] \times 100$$

2.11. In vitro cell studies

2.11.1. Sample preparation

Films were cut aseptically corresponding to 1.5 cm × 1.5 cm and specimens were used directly for testing [32].

2.11.2. Cell viability studies

Viability of the cells was performed using MTT assay. Viability of the cells was assessed using the MTT assay. HEK 293 T cells used for the assay were grown in regular high glucose Dulbeccos Modified Eagles Medium (DMEM) supplemented with 10% fetal bovine serum (FBS) and antibiotic-antimycotic mix. For MTT assay, the cells were resuspended in culture medium and seeded in control wells or wells containing the different films placed in a 96-well plate. The cells were then placed in a humidified atmosphere of 5% CO2 for 24 h or 72 h. Following incubation, the medium was removed and each well was treated with 0.5 mg/ml of 3-(4,5-dime thylthiazol-2-yl)-2,5-diphenyl tetrazolium bromide (MTT) dissolved in DMEM, and incubated for 2 h at 37 °C in a humidified atmosphere of 5% CO2. The yellow MTT is reduced to blue-purple formazan by the mitochondrial dehydrogenase from intact living cells. The resulting blue precipitate was solubilised in DMSO and the absorbance was recorded at 570 nm wavelength using a standard plate reader (Tecan) [32]. Experiments were performed in a triplicate and the data were presented as mean ± SD (n = 3).

The percentage cell viability (CV) was calculated using the formula below:

$$\text{CV}(\%) = (\text{Absorbance of test sample / Absorbance of control}) \times 100$$

3. Results and discussion

3.1. Morphological characteristics of the films

The appearance of the SF, BG and FG films was homogenous, transparent, non-porous and pale yellowish in colour with 60 ± 25 μm thickness. Surface morphology (Fig. 1b, f, i, l, o) and its cross sections (Fig. 1a, d, h, k, n) showed that the blend films or FG films are little rough, uniform without any air bubbles, which proved to be homogeneous and the AFM images (Fig. 1c, g, j, m, p) of the films revealed the change in the roughness value of the blended films at different ratios of SF and BG. The compatibility of SF and BG in blended films was also confirmed through SEM and AFM as seen in Fig. 1.

3.2. Contact angle measurement

The surface wettability of the SF, BG & FG films were analysed using contact analyzer where the water absorption is an important parameter for the wound healing material especially for exudate

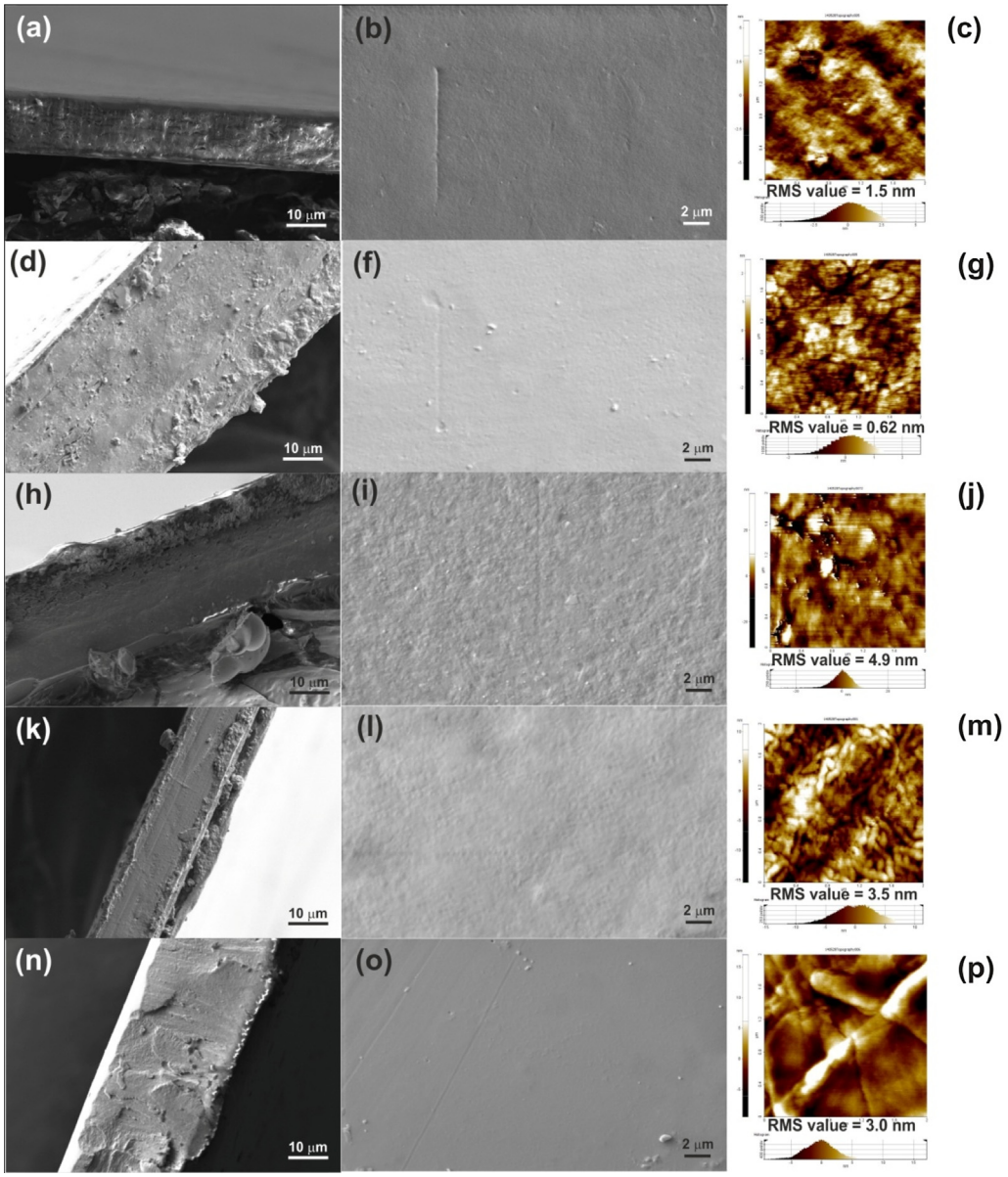

Fig. 1. SEM images of the film with its cross-section and the AFM roughness of each films. (a, d, h, k, n), (b, f, i, l, o) and (c, g, j, m, p) is the SEM image showing cross-section, Surface morphology and AFM image showing surface roughness and RMS value of the SF, FG 75:25, FG 50:50, FG 25:75 and BG respectively.

wounds [33]. Fig. 5 shows the degree of contact angle between 50 and 79°. According to Kwok & Neumann. 2003 [34] the contact angle from 0° to 60° shows high wettability and from 60° to 90° shows moderate wettability. From Fig. 2, the wettability increases by the increase in concentration of BG. Upon blending with BG, the SF wettability increased from moderate to high.

3.3. FTIR characteristics

The structural changes due to the chemical interactions between the fibrous protein and the polysaccharide were determined by IR analysis [35]. Among all the amide bands of proteins, amide band I, II and III are generally selected to differentiate protein structure which were in the range of 1700–1600 cm^{-1}, 1600–1500 cm^{-1} and 1300–1200 cm^{-1} respectively.

BG film exhibited absorption band at 1168 cm^{-1}, 1071 cm^{-1} and 1028 cm^{-1} which corresponds to the CO-CC stretching and COH bending mode present in the sugar region [36]. The Silk Fibroin film has the absorption bands at 1623 cm^{-1} and 1517 cm^{-1} which corresponds to the amide I & amide II linkage of the protein with the β-sheet conformation. The another band at 1231 cm^{-1} corresponds to the amide III linkage of protein with random coil structure [37]. Thus the SF films proved to have both β-sheet and random coil structure simultaneously. The sharp peak at 3280 cm^{-1} (N-H stretching) in the SF film (Fig. 3a) and the appearance of the broad band in BG film (Fig. 3e) is for OH stretching and possess intra- and intermolecular hydrogen bonds. The band in Fig. 3(b–d) showed both pure SF and BG bands with no phase shift but with the intensity difference corresponding to the varying concentration of SF and BG.

3.4. X-Ray diffraction studies

X-Ray diffraction was carried out to study the crystalline structure of the SF/BG blend films. Fig. 3 shows the X-Ray diffraction pattern of the pure and blend SF and BG films. A peak around

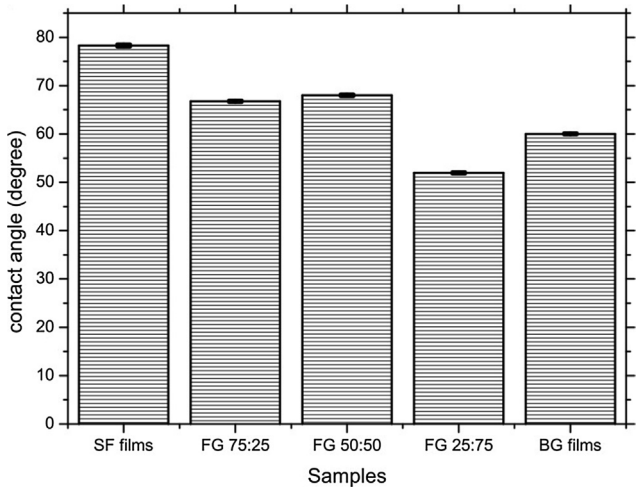

Fig. 2. Contact angle measurement of SF, BG & FG films. Each bar represents mean ± standard error (n = 3).

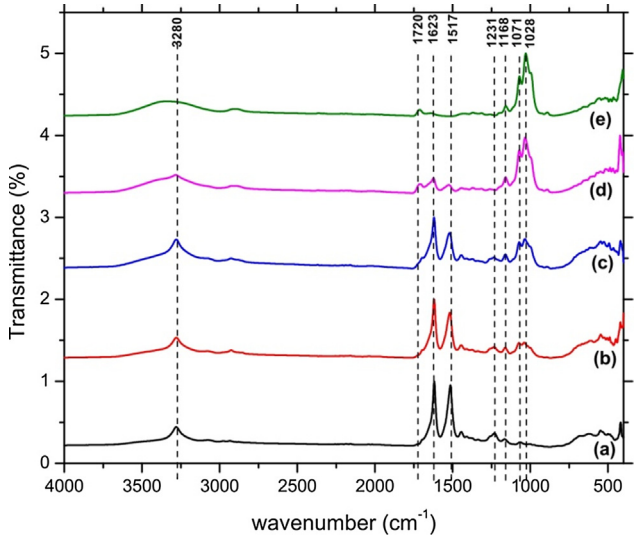

Fig. 3. FTIR spectrum of (a) SF film and SF/BG blend films with various blend ratios of SF & BG (FG) of (b) 75:25, (c) 50:50 (d) 25:75 and (e) BG film.

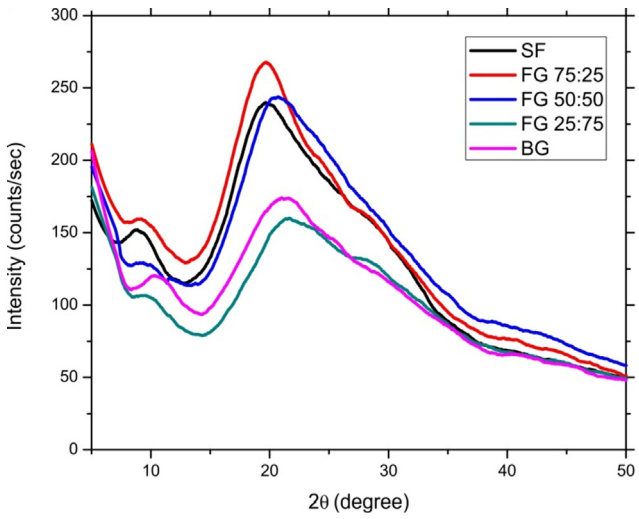

Fig. 4. X-Ray diffraction pattern of SF, BG and FG films.

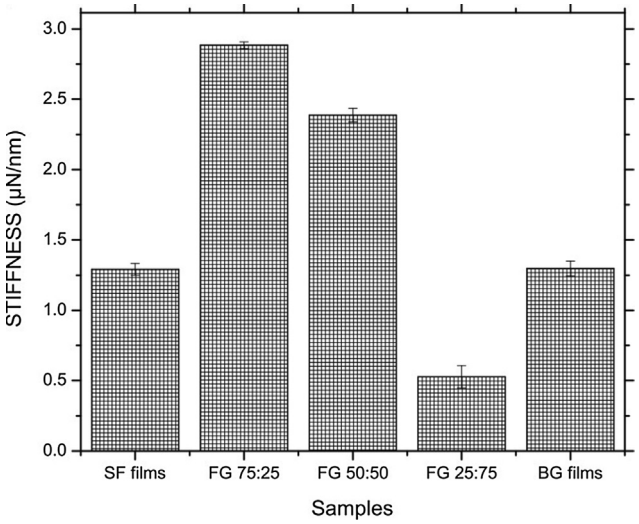

Fig. 5. Stiffness of SF, BG & FG films. Each bar represents mean ± standard error (n = 3).

2θ = 9.2° and 19.5° shown in the Fig. 4 for pure silk fibroin suggests that it is mainly consists of random coil and α-helix conformation with few β-sheet conformation as well. On comparing with the XRD patterns of the microcrystalline polymer [38], these peaks can represent free crystals in micrometer/nanometer size. The peaks around 2θ = 10.6° and 21.6° corresponds to the characteristic peaks of BG. On comparing, both pure SF and BG films, there is no change in the position of the peak but slight shift was shown on blending which might be due to the intermolecular hydrogen bonding. XRD patterns indicate that the crystalline nature of the blends decreased on increasing BG concentration.

3.5. Mechanical studies for stiffness

The stiffness of the ECM can have profound effects on the behaviour of the cells that interact with it [39]. The Stiffness of the SF/BG blend films were studied using indentation technique. Fig. 5 shows that the stiffness of the SF, BG & FG films increases with increase in the silk fibroin ratio.

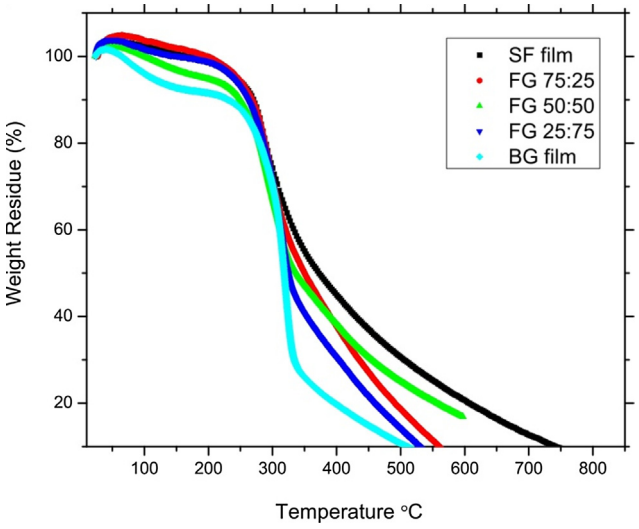

Fig. 6. Thermogravimetric studies of the pure and blended films of SF and BG.

3.6. Degradation studies

3.6.1. Thermogravimetric analysis

Thermal degradation curves of SF, BG & FG films are shown in the Fig. 6. The initial loss below 100 °C was due to the solvent evaporation [40]. In all the peaks, the thermal stability is near to 300 °C. From the curve it is clear that the increase in SF content in the BG increases the degradation temperature proving that SF provides a thermal stability to the blend films.

3.6.2. Water absorption capacity/swelling ratio

Water absorption capacity is one of the important factor for wound dressing material [41]. The absorption capacity of the SF and BG blend films was measured and it was found to be 55–79% of their dry weight (Fig. 7). From the pure BG films the degree of swelling increases with increase in BG content and decreases with increasing the SF content. All prepared blend films retained their form in the aqueous solution as well as after immersion in PBS (pH 7.4) for 24 h.

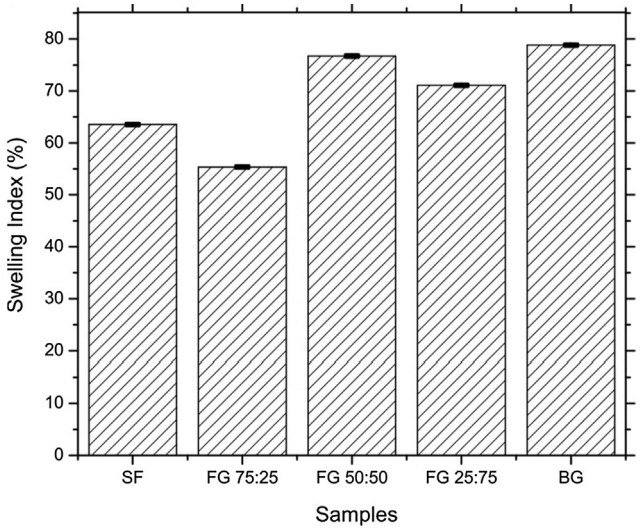

Fig. 7. Swelling property of SF, BG pure films and FG blend films. Each bar represents mean ± standard error (n = 3).

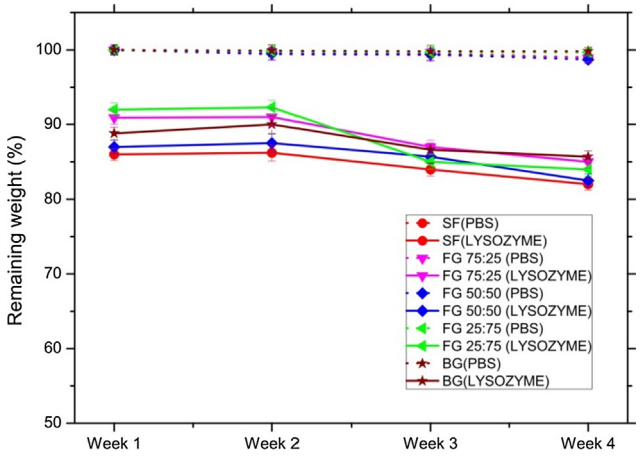

Fig. 8. The percentage of remaining weight of SF, BG films & FG blend films after 4 weeks.

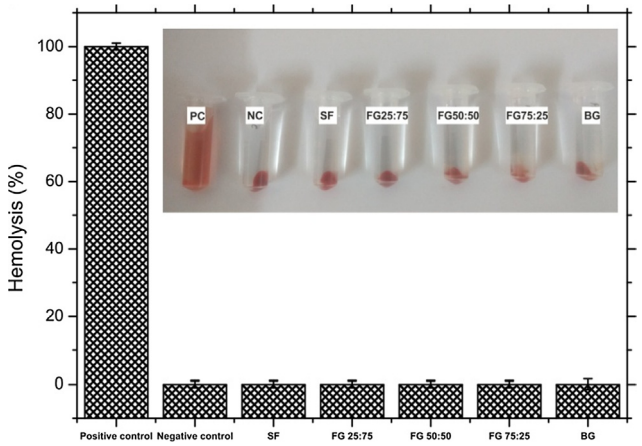

Fig. 9. The percentage of Hemolysis of SF, BG films & FG blend films.

3.6.3. In vitro enzyme degradation

The degradation of SF/BG blend films was studied *in vitro* by degradation with lysozyme enzyme [42], and the remaining weight percentage was determined (Fig. 8) with lysozyme enzyme and PBS as blank. It was found that almost all the samples maintained 80% of their original weight after the incubation of 4 weeks and there was a gradual decrease in weight upto 20% till 3rd week after which the degradation rate decreases subsequently.

3.7. Blood compatibility testing – in vitro hemolytic activity of the films

The Hemolysis testing of films has been used to evaluate the critical interactions of films with blood to explore possible adverse effects arising from the exposure of the SF and BG to blood cells and proteins. Hemolysis rates of pure and the of blend films (Fig. 9) were same as that of negative control which confirms that the films have good blood compatibility and it does not show any traces of lysis of the blood cells [43].

3.8. In vitro cell viability studies

To evaluate the toxicity of the films, we investigated the effect of pure and blended films on the viability of HEK 293 T cells after

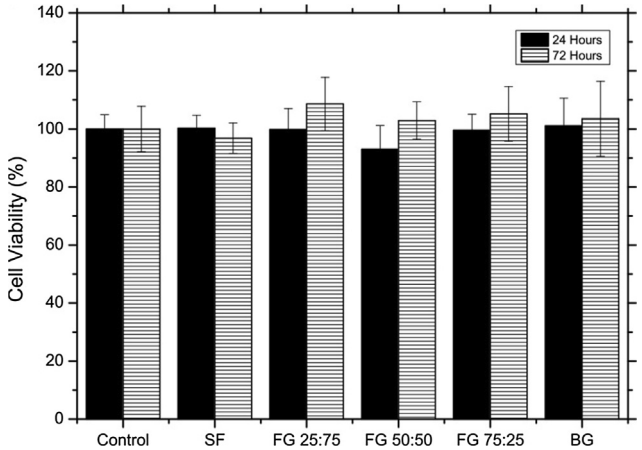

Fig. 10. Cell viability measured by MTT assay following incubation of HEK 293 T cells with pure and blended films for 24 and 72 h. HEK 293 T grown in wells without the films were used as controls.

incubation for 24 and 72 h by MTT reduction assay. As seen in Fig. 10, the pure, as well as the blended films, did not show any noticeable toxicity as the cell viability remained above 90% at 24 and 72 h of incubation when compared to respective controls. [44].

4. Conclusion

This study provided a brief understanding of the physico-chemical interactions between silk fibroin and beta glucan. The SF, BG film and its blends were prepared using formic acid as solvent and various features such as appearance, secondary structure, stiffness and other degradation studies were reported. The Silk fibroin films shows high thermal stability, high hydrophobicity, high stiffness value whereas the paramylon film shows good water absorption property and enzymatic degradation. The blended films show combined nature of silk fibroin and paramylon at different concentrations without any crosslinking or chemical interaction. Thus from the study it may be concluded that silk fibroin acts as a physical barrier by providing high thermal stability and stiffness whereas paramylon acts as a bioactive supplement by boosting water absorption capacity and cell proliferation capacity. Also from the various in vitro studies the hemocompatible and non toxic nature of the prepared film is evident, as more than 90% of viable cells were present in the treated sample. Overall on comparing with other blended films, FG 75:25 shows better property in all experiments and this ratio can further be considered for knowing the actual mechanism in an animal model for the purpose of constructing a self-care wound dressing material.

Appendix A. Supplementary material

Supplementary data to this article can be found online at https://doi.org/10.1016/j.ijbiomac.2019.11.010.

References

[1] C.K. Sen, G.M. Gordillo, S. Roy, R. Kirsner, L. Lambert, T.K. Hunt, F. Gottrup, G.C. Gurtner, M.T. Longaker, Human skin wounds: a major and snowballing threat to public health and the economy, Wound Repair Regener. 17 (2009) 763–771.

[2] J.E.S. Sutcliffe, C. Thrasivoulou, T.E. Serena, L. Madden, T. Richards, A.R.J. Phillips, D.L. Becker, Changes in the extracellular matrix surrounding human chronic wounds revealed by 2-photon imaging, Int. Wound J. 14 (2017) 1225–1236.

[3] Magnus S. Agren, Maria Werthen, The extracellular matrix in wound healing: a closer look at therapeutics for chronic wounds, Int. J. Lower Extremity Wounds 6 (2) (2007) 82–97.

[4] Fa-Ming Chen, Xiaohua Liu, Advancing biomaterials of human origin for tissue engineering, Prog. Polym. Sci. 53 (2016) 86–168.

[5] F.X. Maquart, J.C. Monboisse, Extracellular matrix and wound healing, PathologieBiologie 62 (2) (2014) 91–95.

[6] Dwi Liliek Kusindarta, Hevi Wihadmadyatami, The Role of Extracellular Matrix in Tissue Regeneration', Tissue Regeneration, Intechopen Publishers, London, 2018.

[7] R.I. Kunz, R.M.C. Brancalhao, L.F.C. Ribeiro, M.R.M. Natali, Silkworm Sericin: properties and biomedical applications, BioMed Res. Int. (2016) 1–19.

[8] S. Prasong, S. Yaowalak Wilaiwan, Characteristics of silk fiber with and without Sericin component: a comparison between *Bombyxmori* and *Philosamiaricini* silks, Pak. J. Biol. Sci. 12 (11) (2009) 872–876.

[9] G.H. Altman, F. Diaz, C. Jakuba, T. Calabro, R.L. Horan, J. Chen, H. Lu, J. Richmond, D.L. Kaplan, Silk-based biomaterials, Biomaterials 24 (3) (2003) 401–416.

[10] A. Sugihara, K. Sugiura, H. Morita, T. Ninagawa, K. Tubouchi, R. Tobe, M. Izumiyz, T. Horio, N.G. Abraham, S. Ikehara, Promotive effects of a Silk film on epidermal recovery from full-thickness skin wounds, Proc. Soc. Exp. Biol. Med. 225 (1) (2000) 58–64.

[11] T. Liu, J. Miao, W. Sheng, Y. Xie, Q. Huang, Y. Shan, J. Yang, Cytocompatibility of regenerated silk fibroin film: a medical biomaterial applicable to wound healing, J. Zhejiang Univ. Sci. B 11 (1) (2010) 10–16.

[12] H. Teramoto, T. Kameda, Y. Tamada, Preparation of gel from B. *mori* silk sericin and its characterization as a wound dressing, Biosci. Biotechnol. Biochem. 72 (2008) 3189–3196.

[13] A. Vasconcelos, A.C. Gomes, C. Cavacoo-Paulo, Novel silk fibroin/elastin wound dressing, Acta Biomater. 8 (2012) 3049–3060.

[14] M. Novak, V. Vetvicka, Glucans as biological response modifiers, Endocrine Metabol. Immune Disorders-Drug Targets 9 (1) (2009) 67–75.

[15] F. McCann, E. Carmona, V. Puri, R.E. Pagamo, A.H. Limper, Macrophage internalization of fungal beta-glucan is not necessary for initiation of related inflammatory responses, Infect. Immun. 73 (10) (2005) 6340–6347.

[16] W.L. Wendy Hsiao, Y.Q. Li, T.L. Lee, N. Li, M.M. You, S. Chang, Medicinal mushroom extracts inhibit ras-induced cell transformation and the inhibitory effect requires the presence of normal cells, Carcinogenesis 25 (2004) 1177–1183.

[17] A.B. Onderdonk, R.L. Cisneros, P. Hinkson, G. Ostroff, Anti-infective effect of poly- β-1-6-glucotriosyl-β-1-3-glucopyranose glucan in vivo, Infect. Immun. 60 (1992) 1642–1647.

[18] J.A. Cleary, G.E. Kelly, A.J. Husband, The effect of molecular weight and β-1-6-linkages on priming on macrophage function in mice by (1,3)-β-D glucan, Immunol. Cell Biol. 77 (1999) 395–403.

[19] C.S. Engstad, R.E. Engstad, J.O. Olsen, B. Osteud, The effect of soluble β-1,3-glucan and lipopolysaccharide on cytokine production and coagulation activation in whole blood, Int. Immunopharmacol. 2 (2002) 1585–1597.

[20] S.J. Delatte, J. Evans, A. Hebra, W. Adamson, H.B. Othersen, E.P. Tagge, Effectiveness of beta-glucan collagen for treatment of partial-thickness burns in children, J. Pediatr. Surg. 36 (2001) 113–118.

[21] Antony Bacic, B.F. Geoffrey, A.S. Bruce, Chemistry, Biochemistry and Biology of 1–3 Beta Glucans and Related Polysaccharides, Academic Press, USA, 2009.

[22] Drake RR, Li L & Brown RM 1992, 'Photoaffinitylabeling of cellulose synthases', Proceedings of Cotton Fiber Cellulose: Structure, Function and Utilization Conference, Savannah, Georgia, USA.

[23] L. Barsanti, R. Vismara, V. Passarelli, P. Gualtieri, Paramylon (β-1,3-glucan) content in wild type and WZSL mutant of Euglena gracilis, Effects of growth conditions, J. Appl. Phycol. 13 (2001) 59–65.

[24] Y. Kondo, A. Kato, H. Hojo, S. Nozoe, M. Takeuchi, K. Ochi, Cytokine-related immunopotentiating activities of paramylon, a beta-(1→3)-D-glucan from Euglenegracilis, J. Pharmacobio-dyn. 15 (11) (1992) 617–621.

[25] N. Koizumi, H. Sakagami, A. Utsumi, S. Fujinaga, M. Takeda, K. Asano, I. Sugawara, S. Ichikawa, H. Kondo, S. Mori, K. Miyatake, Y. Nakano, H. Nakashima, T. Murakami, N. Miyano, N. Yamamoto, Anti-HIV (human immune-deficiency virus) activity of sulfatedparamylon, Antiviral Res. 21 (1993) 1–4.

[26] D. Wei, D. Williams, W. Browder, Activation of AP-1 and SP1 correlates with wound growth factor gene expression in glucan-treated human fibroblasts, Int. Immunopharmacol. 2 (8) (2002) 1163–1172, https://doi.org/10.1016/S1567-5769(02)00082-6.

[27] M. Berdal, H.I. Appelbom, J.H. Eikrem, A. Lund, S. Zykova, L.T. Busund, R. Seljelid, T. Jenssen, Aminated β-1,3-D-glucan improves wound healing in diabetic *db/db* mice, Wound Repair Regener. 15 (2007) 825–832.

[28] D.N. Rockwood, R.C. Preda, T. Yucel, X. Wang, M.L. Lovett, D.L. Kaplan, Material fabrication from bombyx mori silk fibroin, Nat. Protoc. 6 (10) (2011) 1614–1631.

[29] N. Nwe, T. Furuike, H. Tamura, The mechanical and biological properties of chitosan scaffolds for tissue regeneration templates are significantly enhanced by chitosan from *gongronellabutleri*, Materials 2 (2) (2009) 374–398.

[30] Suvama Kurhade, Munira Momin, Pallavi Khanekar, Supriya Mhatre, Novel biocompatible honey hydrogel wound healing sponge for chronic ulcers, Int. J. Drug Deliv. 5 (2013) 353–361.

[31] Seung Il Kim, Bo Ram Lee, Jin Ik Lim, Cho Hay Mun, Youngmee Jung, Ji-Heung Kim, Soo Hyun Kim, Preparation of topographically modified poly(L-lactic acid)-b-poly(ε-caprolactone)-b-poly(L-lactic acid) tri-block copolymer film surfaces and its blood compatibility, Macromol. Res. 22 (11) (2014) 1229–1237.

[32] Cornelia Wiegand, Martin Abel, Uta-Christina Hipler, Peter Elsner, Effect of non-adhering dressing on promotion of fibroblast proliferation and wound healing *in vitro*, Sci. Rep. 9 (1) (2019) 4320–4329.

[33] P. Zahedi, I. Rezaeian, S. Ranaei-Siadat, S. Jafari, P. Supaphol, A review on wound dressings with an emphasis on electrospunnanofibrous polymeric bandages, Polym. Adv. Technol. 21 (2010) 77–95.

[34] D.Y. Kwok, A.W. Neumann, Contact Angle, Wettability and Adhesion 3 (2003) 117.

[35] T. Hino, M. Tanimoto, S. Shimabayashi, Change in secondary structure of silk fibroin during preparation of its microsphere by spray-drying and exposure to humid atmosphere, J. Colloid Interface Sci. 266 (2003) 68–73.

[36] A. Synytsya, M. Novak, Structural analysis of glucans, Annu. Transl. Med. 2 (2014) 17.

[37] S.W. Ha, A.E. Tonelli, S.M. Hudson, Structural studies of Bombyxmori silk fibroin during regeneration from solutions and wet fiber spinning, Biomacromolecules 6 (3) (2005) 1722–1731.

[38] D. Ciolacu, F. Cliolacu, V. Popa, Amorphous cellulose – structure and characterization, Cellulose Chem. Technol. 45 (2011) 13–21.

[39] A.M. Handorf, Y. Zhou, M.A. Halanski, W. Li, Tissue stiffness dictates development, homeostasis and disease progressin, Organogenesis 11 (1) (2015) 1–15.

[40] M.A. Moraes, G.M. Nogueira, R.F. Weska, M.M. Beppu, Preparation and characterization of insoluble silk fibroin/chitosan blend films, Polymers 2 (2010) 719–727.

[41] E.A. Kamoun, E.S. Kenawy, X. Chen, A review on polymeric hydrogel membranes for wound dressing applications: PVA-based hydrogel dressing, J. Adv. Res. 8 (3) (2017) 217–233.
[42] T. Siritientong, J. Ratanavaraporn, T. Srichana, P. Aramwit, Preliminary characterization of genepin-cross-linked silk sericin/poly(vinyl alcohol) films as two-dimensional wound dressings for the healing of superficial wounds, BioMed Res. Int. (2013) 1–13.
[43] Angelica Panico, Federica Paladina, Mauro Pollini, Development of regenerative and flexible fibroin-based wound dressing, J. Biomed. Mater. Res. Part-B Appl. Biomater. 107 (1) (2018) 7–18.
[44] Katyakyini Muniandy, Sivapragasam Gothai, Woan Sean Tan, S. Suresh Kumar, Norhaizan Mohd Esa, Govindasamy Chandramohan, Khalid S. Al-Numair, Palanisamy Arulselvan, In vitro wound healing potential of stem extract of Alternanthera sessilis, Evid.-based Complement. Altern. Med. 2018 (2018) 1–13.